ECS Journal of Solid State Science and Technology

You may also like

- Swift heavy ion irradiation induced microstructural modification and evolution of photoluminescence from Si rich *a*-SiN_x:H
R K Bommali, S Ghosh, G Vijaya Prakash et al.

- Non-chemical fluorination of hexagonal boron nitride by high-energy ion irradiation
Shiro Entani, Konstantin V Larionov, Zakhar I Popov et al.

- Engineering NiO Thin Film Properties using Ag^{9+} Ion Irradiation at Various Fluences
Karishma, Neeti Tripathi, Ambuj Tripathi et al.

Impacts of Low Energy Argon Beam on Enhancing the Surface Wettability and Electrical Performance of CA/PANI Films

To cite this article: Reem Altuijri *et al* 2024 *ECS J. Solid State Sci. Technol.* **13** 043017

View the article online for updates and enhancements.

PAT-Tester-x-8 Potentiostat:
Modular Solution for Electrochemical Testing!

EL-CELL®
electrochemical test equipment

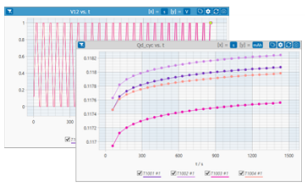

- **Flexible Setup with up to 8 Independent Test Channels!**
  Each with a fully equipped Potentiostat, Galvanostat and EIS!
- **Perfect Choice for Small-Scale and Special Purpose Testing!**
  Suited for all 3-electrode, optical, dilatometry or force test cells from EL-CELL.
- **Complete Solution with Extensive Software!**
  Plan, conduct and analyze experiments with EL-Software.
- **Small Footprint, Easy to Setup and Operate!**
  Usable inside a glove box. Full multi-user, multi-device control via LAN.

Scan me!

Contact us:
+49 40 79012-734
sales@el-cell.com
www.el-cell.com

This content was downloaded from IP address 165.132.5.150 on 26/04/2025 at 09:34

ECS Journal of Solid State Science and Technology, 2024 **13** 043017
2162-8777/2024/13(4)/043017/9/$40.00 © 2024 The Electrochemical Society ("ECS"). Published on behalf of ECS by IOP Publishing Limited

Impacts of Low Energy Argon Beam on Enhancing the Surface Wettability and Electrical Performance of CA/PANI Films

Reem Altuijri,[1] A. Atta,[2,z] E. Abdeltwab,[2] and M. M. Abdelhamied[3]

[1]*Department of Physics, College of Science, Princess Nourah bint Abdulrahman University, P O Box 84428, Riyadh 11671, Saudi Arabia*
[2]*Physics Department, College of Science, Jouf University, Sakaka, Saudi Arabia*
[3]*Radiation Physics Department, National Center for Radiation Research and Technology (NCRRT), Egyptian Atomic Energy Authority (EAEA), Cairo, Egypt*

This work study the impacts of argon irradiation on surface wettability of CA/PANI using home made ion source with fluences (4×10^{14}, 8×10^{14}, and 12×10^{14} ions cm^{-2}). The EDX, SEM and FTIR methods verified the successful fabrication of the composites. Surface wettability, contact angle, and work of adhesion were measured for the untreated and irradiated composites. Raising the ion flux from 4×10^{14} ions.cm^{-2} to 12×10^{14} ions.cm^{-2}, it decreases the contact angle of CA/PANI from 62.1° to 43.4° and increases the surface free energy from 46.7 to 63.9 mJ m^{-2}. The results showed that the CA/PANI changed after exposed to radiation, proving that the irradiated surface properties were improved. In addition, their electrical conductivity was tested in frequency of 50 to10^6 Hz. When subjected to 12×10^{14} ions.cm^{-2}, the conductivity rose from 1.1×10^{-8} S cm^{-1} for CA/PANI to 6.5×10^{-7} S cm^{-1}. The results showed that the irradiated CA/PANI had better electrical and surface properties, which is crucial for many devices including batteries and supercapacitors.
© 2024 The Electrochemical Society ("ECS"). Published on behalf of ECS by IOP Publishing Limited. [DOI: 10.1149/2162-8777/ad405a]

Manuscript submitted March 1, 2024; revised manuscript received April 11, 2024. Published April 29, 2024.

Polymer nanocomposites materials are highly versatile and possess unique features that make them an important part of modern materials in fields of research and engineering.[1,2] Research into nanocomposite materials is focused on enhancing the efficiency and performance of energy conversion technologies, including fuel cells and photovoltaics, as well as energy storage systems.[3,4] Their capacity to merge the adaptability of polymers with the distinct characteristics of nanofillers paves the way for innovation in several fields. With their improved electrical conductivity, thermal management, and electromagnetic interference capabilities, nanocomposite materials find widespread application in electronic devices, printed circuit boards, and conductive coatings.[5,6]

Polymeric material cellouse acetate have a notable characteristics can be tailored to be used in a wide range of industries.[7] The biopolymer cellulose with exceptional characteristics is created when cellulose is acetylated to form cellulose acetate.[8] Because of its biodegradability, cellulose acetate is an eco-friendly substance, which is one of its notable properties.[9] Cellulose acetate has sustainability features make it a versatile material that finds usage in coatings, adhesives, and the creation of thin films.[10] Some biomedical uses, like drug delivery devices and wound dressings, are suited to cellulose acetate because of its biodegradability and biocompatibility.[11]

The unique properties of polyaniline (PANI) make it an attractive material for use in a wide range of industries, making it one of the most prominent polymers.[12] Many researcher are interested in polyaniline because of its unusual electrical, thermal, and redox characteristics.[13] Given its conductive properties, PANI has proven to be an adaptable material with numerous uses. Conductive PANI fillers find usage in a variety of applications, including detectors and sensors Changes to the CA/PANI composite's characteristics were necessary because of these materials have many uses in the textile and coating industries.[14] The chemical and structural characteristics of CA polymeric materials are changed when PANI filler is added to them. Since PANI is electrically conductive, and have great promise as a component of flexible electronic components.[15]

The use of irradiation to modify the surface and electrical characteristics of polymer composites paves the way for their incorporation into various electronic devices and sensors.[16,17] Ion beam irradiation allows polymer composites to gain improved mechanical characteristics and thermal stability, which opens up new possibilities for their usage in energy components.[18] Using low-energy ion beam irradiation to modify polymer composites could be a great way to make these materials work better for certain uses.[19] Furthermore, by analyzing their electrical conductivity, the irradiatied samples were shown to be suitable for application in energy storage devices.[20]

Using environmentally friendly ion beam irradiation to alter the CA/PANI surface characteristics, electrical conductivity, and structural composition is the innovative part of this work. The flexible nanocomposite films were also analyzed using different techniques such as EDX, SEM, and FTIR. Contact angle measurements show that the ion beam improves the surface's wettability. Modifying the ion source parameters is the unique contribution of this study to the management of CA/PANI films for application in biosensors and solar cells. In addition, ion beam irradiation will introduce vacancies and structural alterations within the CA/PANI films. Furthermore, the effect of an argon beam on the electrical conductivity of CA/PANI was ascertained. The findings indicate that the samples that were exposed to radiation were modified in a way that makes them suitable for usage as both coatings and supercapacitors.

Experimental Work

The solution casting method was utilized, as previously reported in the fabrication of the CA/PANI folms.[21] The PANI suspensions were prepared by dissolving 0.15 g of PANI in 8 ml of DMF using the ultrasonic probe. The composite film made of CA and PANI was cast using a solvent. The liquid was agitated at room temperature for two hours to achieve dispersion. After that, the mixture was moved into a petri dish made of glass to be sure all the solvents had evaporated. The CA/PANI composite samples were irradiated by Argon beam at fluencies of 4×10^{14} ions cm^{-2}, 8×10^{14} ions cm^{-2}, and 12×10^{14} ions cm^{-2}. This low fluence is useful for technically induced changes in composite materials, as indicated before.[17–21] Additionally, the films' structural integrity can be compromised at fluence levels exceeding certain thresholds. The Ar+ beam was extracted using the hand-made ion source as previously reported,[22] as seen in Fig. 1. The CA/PANI films were subjected to an argon beam of 4 keV energy, and 182 $\mu A/cm^2$ current. The low-energy structural effects are determined by variations in the beam properties. And the high-energy is breaks down the polymer structure. The vibrational groups and chemical composition of the original CA/PANI composite film were examined in by FTIR in frequency range of 400–4000 cm^{-1} range. In order to record the conductivity at

[z]E-mail: aamahmad@ju.edu.sa

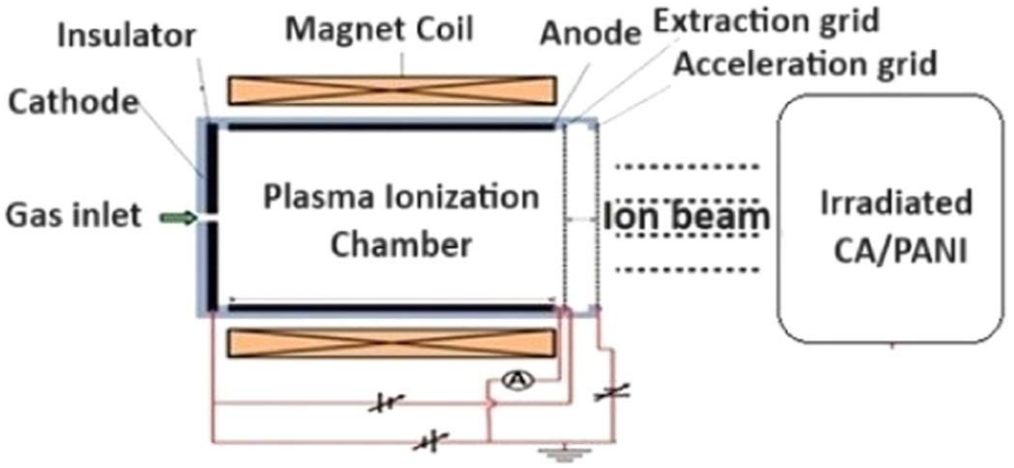

Figure 1. A broad beam low energy ion source.

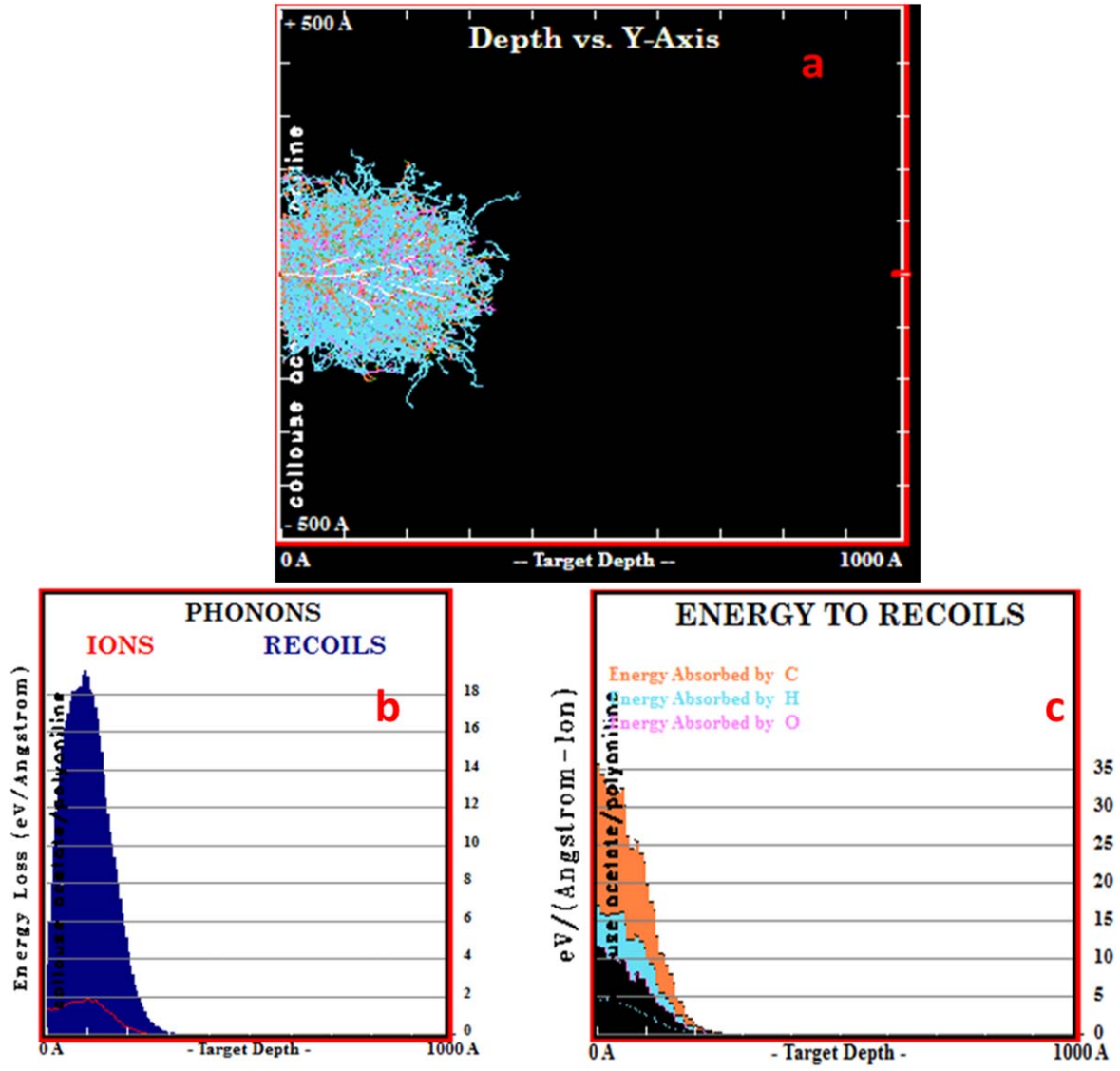

Figure 2. (a) Ar ions interaction with CA/PANI, and (b) recoiled atoms to phonons of Ar ions with CA/PANI, (c) energy to recoils of Ar ions in CA/PANI.

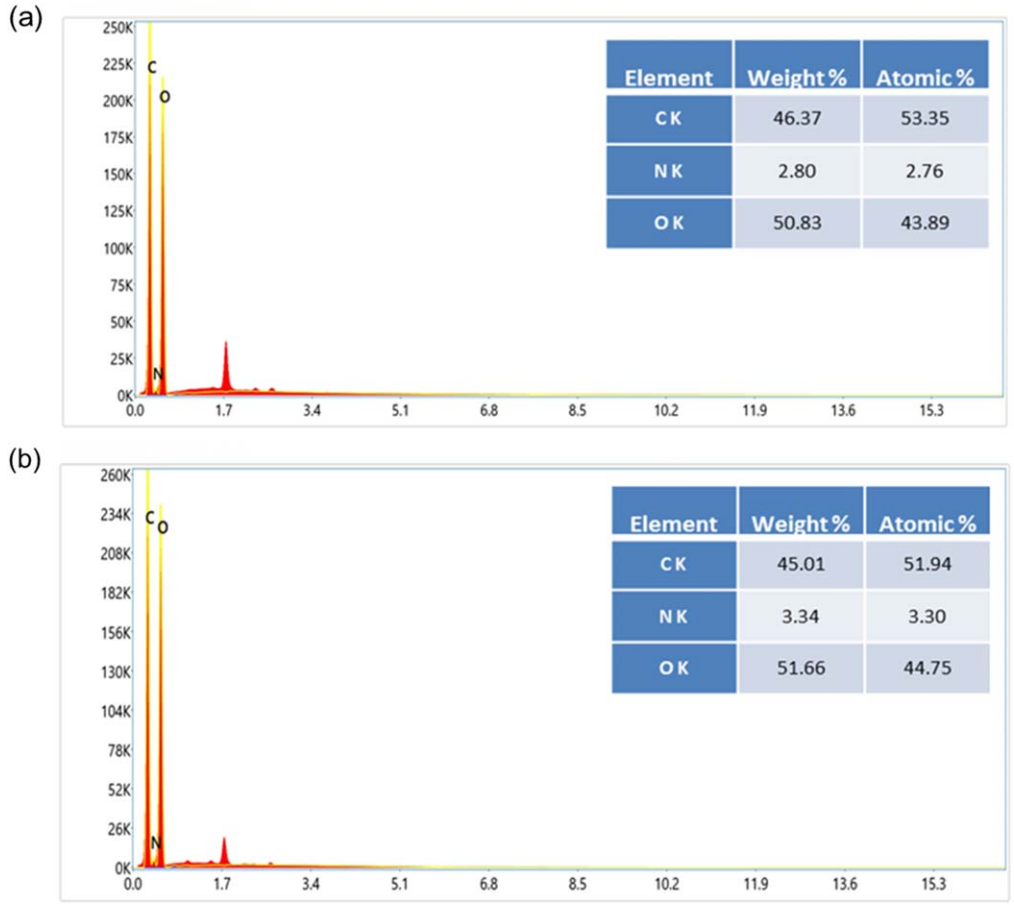

Figure 3. EDX of (a) the CA/PANI and (b) irradiated CA/PANI films by 8×10^{14} ions cm^{-2}.

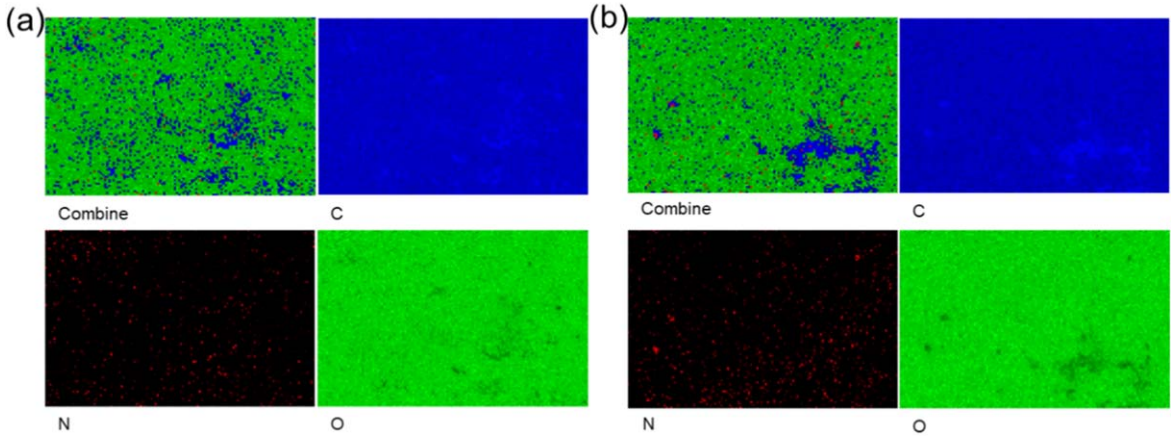

Figure 4. Mapping of (a) the CA/PANI and (b) irradiated CA/PANI films by 8×10^{14} ions cm^{-2}.

frequency range of 50 Hz to 5.5 MHz, the LCR bridge meter (RS-232C, Japan) is used. The interaction between free charge polarization is strongest in this frequency band. Because of the crucial role that interfacial relaxation plays in producing significant structural defects.

Results and Discussion

Ion irradiation is a powerful method for controlling and improving the properties of CA/PANI samples. The SRIM simulation program[23] is used to study the process of surface modification of ion irradiated CA/PANI. The simulation program is used to investigate the informations of range and ion distribution as indicated in Fig. 2. The collected data from the interaction of 4 keV argon ions hitting CA/PANI at depths of 0 to 1 um is shown in the Fig. 2a. The phonos process of the target atoms is illustrated in Fig. 2b. Atoms that have recoiled in the target send less argon ions to the phonos. Figure 2c shows that atoms can utilise the energy they receive from ion bounces to escape the framework and attack adjacent atoms.[24]

For further invesitigation, the EDX analyses were also utilized to confirm the incorporation of PANI with CA polymer and to record the influence of argon beam on the weight percentage of component elements of the composite. Figures 3a, 3b represents the EDX

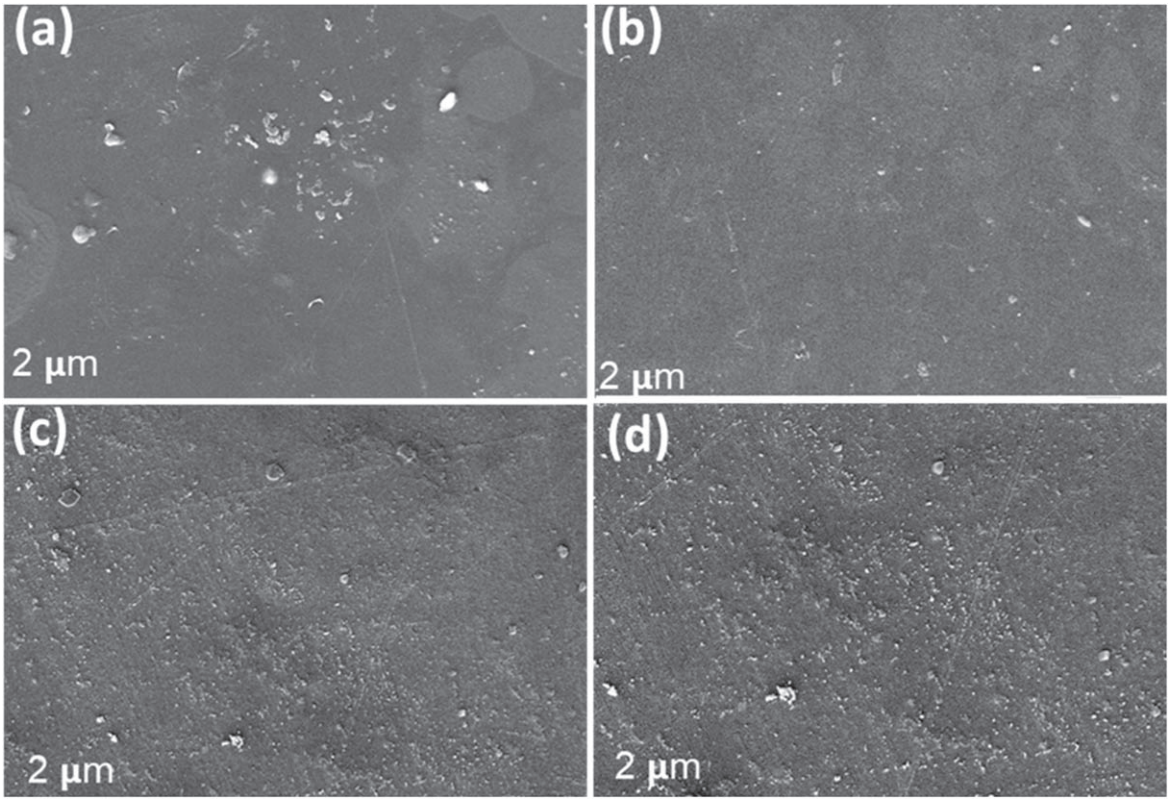

Figure 5. SEM of (a) CA/PANI, (b) 4×10^{14} ions cm^{-2}, (c) 8×10^{14} ions cm^{-2} and (d) 12×10^{14} ions cm^{-2}.

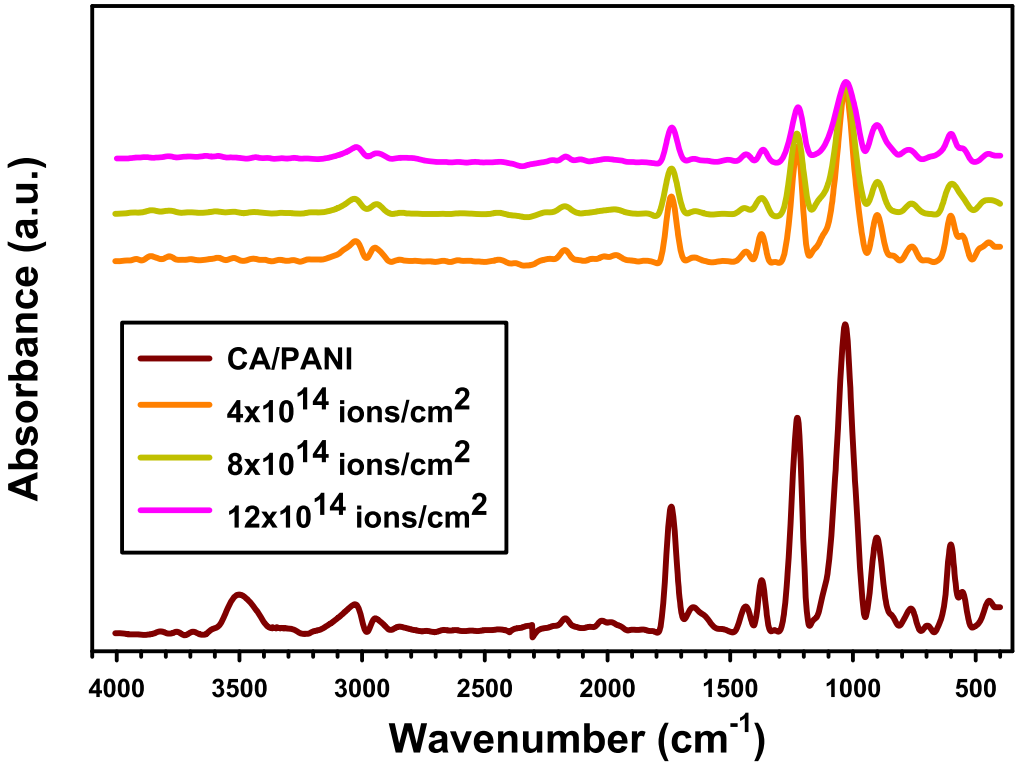

Figure 6. FTIR spectra of the pristine and irradiated CA/PANI composite films.

elemental analysis of the pristine and treated films by 8×10^{14} ions cm^{-2}, respectively. From Fig. 3a, it can be noticed that the spectrum shows characteristic elemental peaks of carbon (C), oxygen (O), and nitrogen (N), confirming the presence of CA and PANI in the CA/PANI composite. After treatement as seen in Fig. 3b, the spectrum reveals that the weight percentage of component elements is changed because the interaction of ion irradiation with the samples.[25]

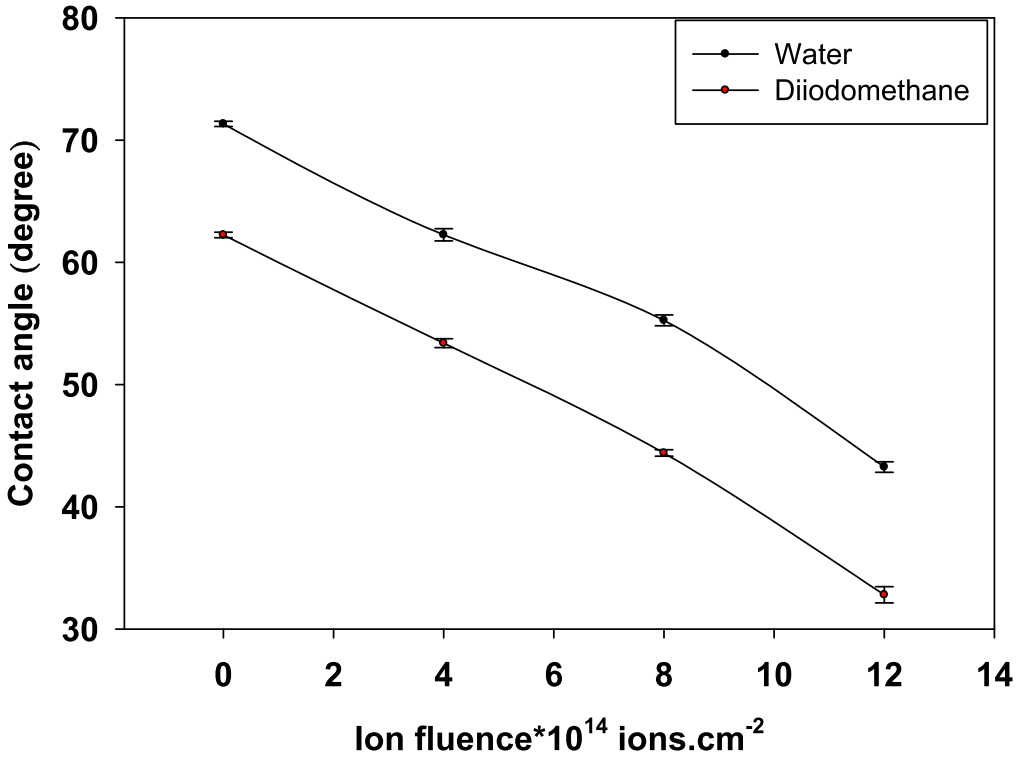

Figure 7. The contact angle for pure and treated CA/PANI.

Table I. The θ and W_a for pure and treated CA/PANI.

	Contact angle θ		Work of adhesion W_a	
	Water	Diiodomethane	Water	Diiodomethane
CA/PANI	71.3	62.2	95.1	74.4
4×10^{14} ions cm^{-2}	62.1	53.3	105.5	81.1
8×10^{14} ions cm^{-2}	55.2	44.4	113.5	87.9
12×10^{14} ions cm^{-2}	43.4	32.8	124.6	93.4

The element mapping of the CA/PANI before and after irradiation was employed in Fig. 4. The mapping spectrum of the pristine CA/PANI is displayed in Fig. 4a. The figure shows that the carbon (C), nitrogen (N), and oxygen (O) enriched areas of the composite with contents weight of 46.37, 2.8, and 50.83% respectively. It can also be seen that the elements are distributed in the composite. In which, the presence of the C and O atoms proved the existence of cellose acetate, while the presence of N confirmed the formation of PANI. Figure 4b presents the elemental mapping of the CA/PANI composite film after irradiation by 8×10^{14} ions cm^{-2}. It is clear that the composite's elemental distribution changed, and that the components' contents weight ranged from 45.01% C, 3.34% N, and 51.66% O. These changes is attributed to the oxidation reactions, the chain scission and the formation of free radicals.[26]

Figures 5a–5d displays the morphology of both the untreated and irradiated CA/PANI composites (a-d). Figure 5a shows the PANI organized in a granular shape within the CA matrix, with white dots dispersed across the CA surface. The next treatment with ion fluxes of 4×10^{14}, 8×10^{14}, and 12×10^{14} ions cm^{-2} also shows considerable morphological alterations as shown in Fig. 5b–5d. The micrographs of the exposed films demonstrated that the CA reacts more strongly with the PANI. Irradiated films develop scission chains and a rough texture. The surface roughness is caused by the Ar+ beam. The because the PANI particles is changed when exposed to ions.[27]

Figure 6 displays the FTIR of untreated and treated CA/PANI at fluences of 4×10^{14}, 8×10^{14}, and 12×10^{14} ions cm^{-2}. The O-H and the C-H bonding are indicated by the absorbance bands respectively at approximately 3497 cm^{-1} and 3033 cm^{-1}, in the CA/PANI. There is band at 1741 cm^{-1} for ester -C=O link, and another at 1375 cm^{-1} that represents the C-H bond. These bands suggest that the cellulose has undergone acetylation.[28] In addition, the carboxylate group of C-O-C rings is indicated by a strong peak at 1230 cm^{-1}, while the pyranose ring is observed at 1035 cm^{-1}. Irradiated CA/PANI exhibits a decreasing FTIR peak intensity with increasing ion irradiation. The interaction between the ion beam and CA/PANI is typically responsible for this decrease.[29] An additional benefit of irradiation is an improvement in the visible properties of the irradiated composite, as seen by the bands shifting after irradiation. Additionally, it observed that the irradiated CA/PANI films' band positions shifted due to chain degradation.

Figure 7 displays the relationship between the ion bombardment and contact angle of CA/PANI in for diiodomethane and water. The contact angle for CA/PANI decreases gradually with increasing ion exposure as in in Table I. The contact angle is reduced from 62.1° to 43.4° for water and for the diiodomethane is reduced from 53.3° to 32.8°, by varying the ion fluence from 4×10^{14} ions.cm^{-2} to 12×10^{14} ions.cm^{-2}. When CA/PANI surfaces are subjected to ion irradiation, the contact angle of water and diiodomethane was decrease depending on the ion fluence. Ion irradiation can lead to

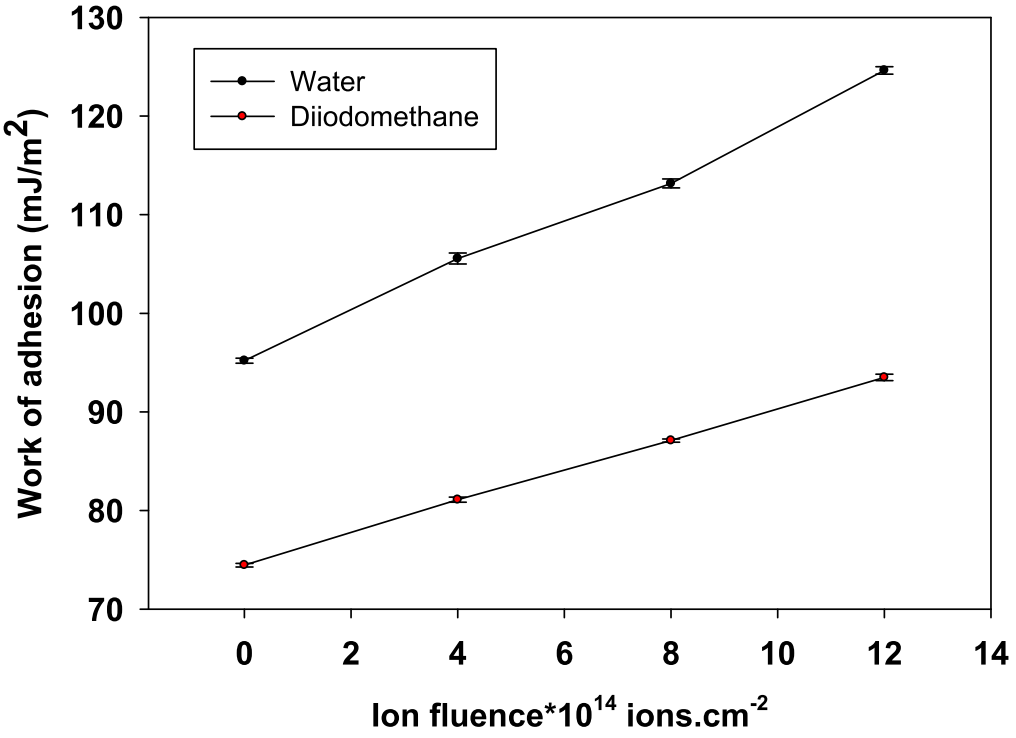

Figure 8. The adhesion work for pure and treated CA/PANI.

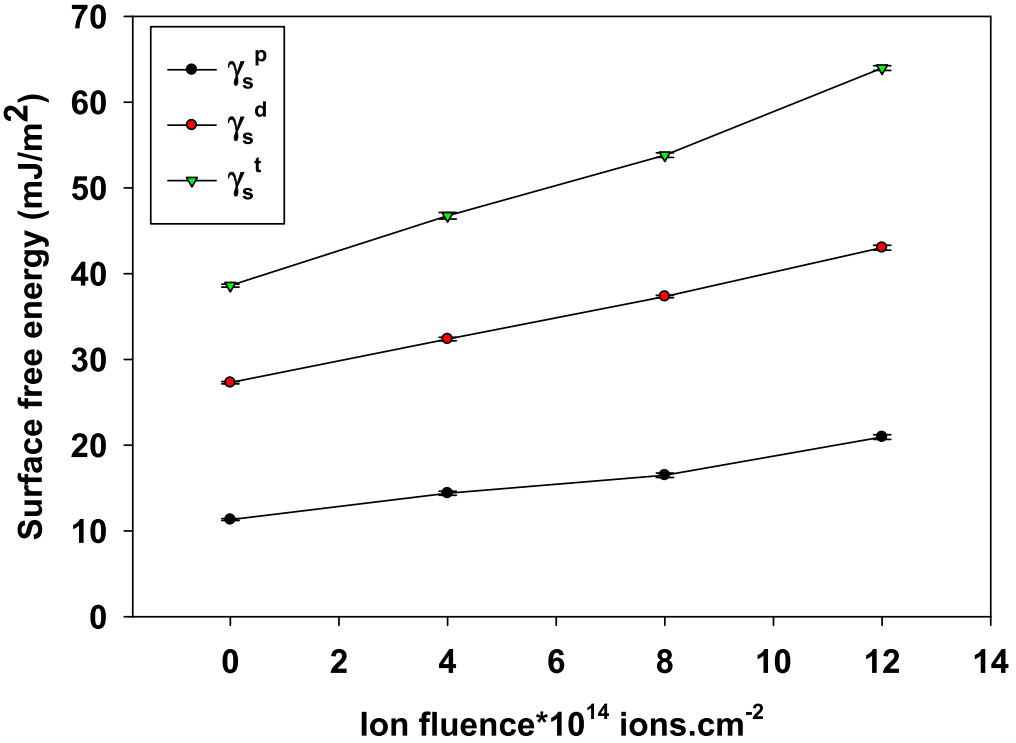

Figure 9. The surface free energy for pure and treated CA/PANI.

surface modification, such as the creation of surface roughness, introduction of functional groups, or alteration of surface tension.[30] These changes can affect the wetting behavior of the polymer surface.[31]

The adhesion work (W_a) is determined by the next formula using the surface free energy of the liquid (γ_l) by.[32]

$$W_a = \gamma_l(1 + \cos\theta) \quad [1]$$

The adhesion work with ion fluence is plotted in Fig. 8. The W_a is raised from 74.2 to 130.4 mJ/m^2 for water, and for diiodomethane enhanced from 68.4 to 95.5 mJ m^{-2} by increasing ion

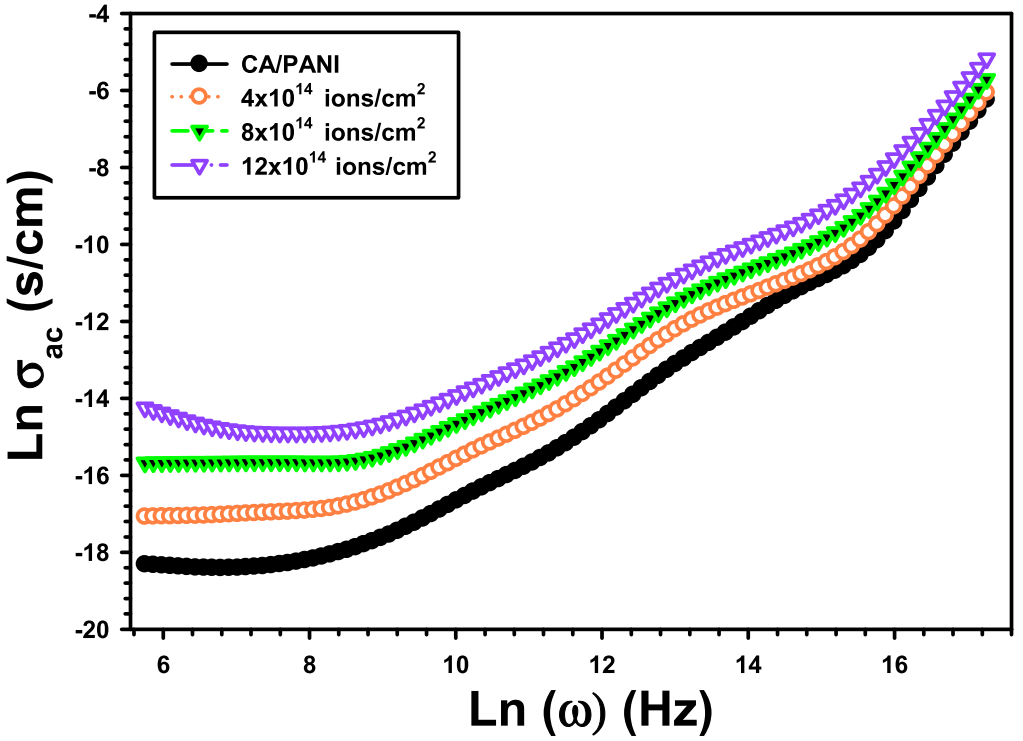

Figure 10. σ_{ac} for pure and treated CA/PANI.

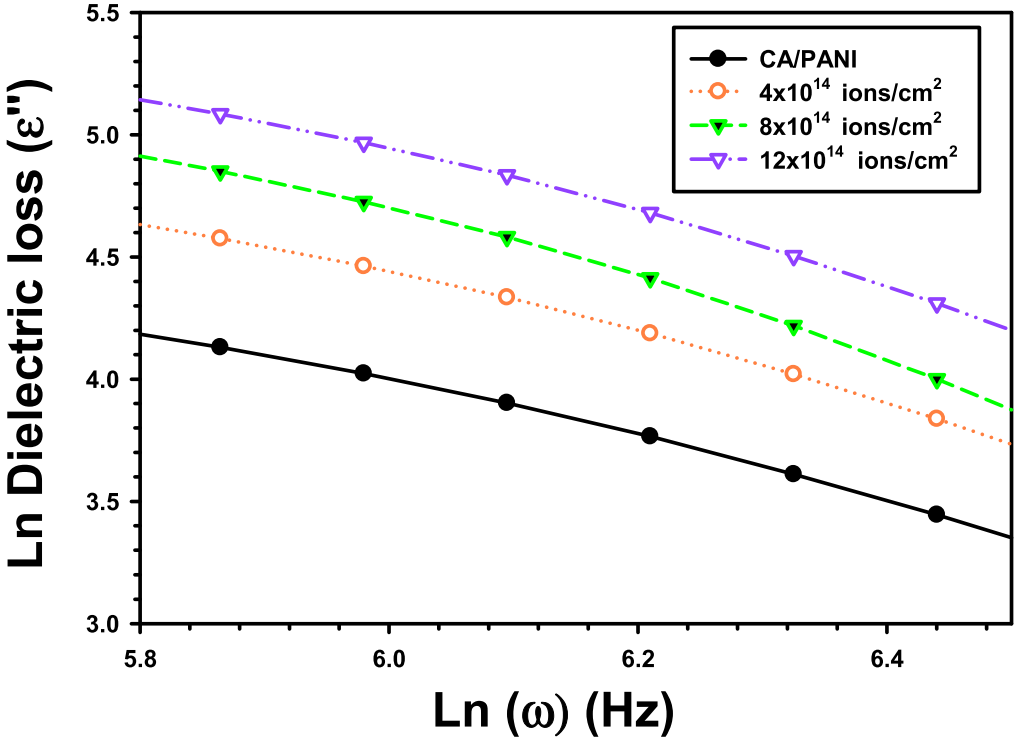

Figure 11. Variation of Ln (ε'') versus Ln (ω) for pure and treated CA/PANI.

fluence from 4×10^{14} to 4×10^{14} ions.cm^{-2} as seen in Table I. This increase in the work of adhesion of CA/PANI by irradiation, resulting from the reduction in the liquid contact angle.[33] This means that water spreads more easily on the surface, indicating increased hydrophilicity.[34]

The surface free energy is given by.[35]

$$\frac{\gamma_l(1+\cos\theta)}{2\sqrt{\gamma_l^d}} = \sqrt{\gamma_s^d} + \sqrt{\gamma_s^p}.\sqrt{\frac{\gamma_l^p}{\gamma_l^d}} \quad [2]$$

Table II. The γ_s^p, γ_s^d, and γ_s^t for pure and treated CA/PANI.

	Polar γ_s^p (mJ/m^2)	Dispersive γ_s^d(mJ/m^2)	total γ_s^t (mJ/m^2)
CA/PANI	11.3	27.2	38.6
4×10^{14} ions cm^{-2}	14.3	32.3	46.7
8×10^{14} ions cm^{-2}	16.4	37.3	53.8
12×10^{14} ions cm^{-2}	20.9	43.1	63.9

Where, the interfacial tensions of solid vapor is γ_s, for solid-liquid is γ_{sl}, and for liquid-vapor is γ_l. Figure 9 show the polar γ_s^p, dispersive γ_s^d, and total γ_s^t surface free energy with ion fluence. The γ_s^d is enhanced from 32.3 to 43.1 mJ m^{-2}, the γ_s^p is enhanced from 14.3 to 20.9 mJ m^{-2} and the γ_s^t is enhanced from 46.7 mJ m^{-2} to 63.9 mJ m^{-2} , as seen in Table II, by raising the ion fluence of 4×10^{14} to 12×10^{14} ions.cm^{-2}. The oxidation process and the chemical changes are the responsible for this behaviour.[36,37] The development of polar fuction is the primary cause of the rise in surface free energy, which includes both the dispersive and polar components.[38]

The σ_{ac} is estimated by the next formulat.[39]

$$\sigma_{ac} = 2\pi f \epsilon_o \epsilon'' \quad [3]$$

Where are $\boldsymbol{\varepsilon''}$ is the dielectric loss and $\boldsymbol{\varepsilon_o}$ is free space permittivity. Figure 10 displays the $\ln(\sigma_{ac})$ with $\ln(\omega)$ for CA/PANI films. Particularly, the conductivity of all the films improves with frequency. As the bond begins to spin, a dielectric transition and complicated charge transfer are formed. At applied frequency 50 Hz, the σ_{ac} increases from 1.1×10^{-8} S.cm^{-1} for un-irradiated CA/PANI to 3.8×10^{-7} S.cm^{-1} for 4×10^{14} ions.cm^{-2}, to 4.6×10^{-7} S.cm^{-1} for 8×10^{14} ions.cm^{-2} and reaches 6.5×10^{-7} S.cm^{-1} for 12×10^{14} ions.cm^{-2}. This is due to the fact that irradiation will break the polymer chain, allowing ions and electrons to flow more freely. Free radicals are also produced in the chain by ion irradiation, which changes the orientation of the dipole. Additionally, the induced polarization is responsible for the increase in electrical conductivity caused by ion irradiation. The induced scission and homopolar connections in the irradiated samples are those responsible for this polarization.

The next formula[40] is used to compute the maximum potential barrier W_M.

$$W_m = \frac{-4k_B T}{m} \quad [4]$$

The following formula is used to compute m from the slope of Ln ($\boldsymbol{\varepsilon''}$) vs Ln ($\omega$) displayed in Fig. 11, where k_B is the Boltzmann constant and T is the room temperature.[41]

$$\varepsilon'' = A\omega^m \quad [5]$$

The estimated value decreased from 0.116 eV for pure CA/PANI to 0.11 eV for 4×10^{14} ions.cm^{-2} to 1.07 eV for 8×10^{14} ions.cm^{-2}, and to 1.03 eV for 12×10^{14} ions.cm^{-2}. Previously, the FTIR data showed that the produced defects in the chains structure is caused by ion bombardment. This because a more disordered microstructure is formed after ion irradiation. Furthermore, as ion irradiation increases, more defects and scission were produced in the treated sample compared to the pure sample.

Conclusions

In the present study, CA/PANI hybrid films were produced using the solution casting reducing approach. The FTIR, EDX and SEM confirmed the successful preparation of CA/PANI. The samples were exposed to different fluencies of ion beam using a handmade ion source. Surface wettability and electrical conductivity of CA/PANI were examined in relation to ion beam irradiation. By means of the SRIM Monte Carlo simulation programme, the electronic/nuclear stopping energy distribution and the ion range are computed. The surface free energy γ_s^t is improved from 46.7 mJ m^{-2} to 63.9 mJ m^{-2} by raise the fluence from 4×10^{14} to 12×10^{14} ions cm^{-2}. Furthermore the electrical characteristics in determined in frequency of 50 Hz to 5.5 MHz. the electrical conductivity at frequency of 50 Hz, increased from 3.8×10^{-7} S.cm^{-1} for CA/PANI to 6.5×10^{-7} for irradiated films by 12×10^{14} ions cm^{-2}. These findings open up new possibilities for using irradiated CA/PANI in different applications. As a result of significant changes to its chemical, surface wettability and structural properties, the irradiated CA/PANI samples are now more useful in various coating applications. In adittion, the improvement in the electrical properties as indicated by the obtained results offer new opportunities to apply the irradiated CA/PANI composites in battery and super capacitor applicationsin.

Acknowledgments

Princess Nourah bint Abdulrahman University Researchers Supporting Project number (PNURSP2024R399), Princess Nourah bint Abdulrahman University, Riyadh, Saudi Arabia.

ORCID

A. Atta https://orcid.org/0000-0001-9451-6777

References

1. A. Atta, H. Negm, E. Abdeltwab, M. Rabia, and M. M. Abdelhamied, "Facile fabrication of polypyrrole/NiOx core-shell nanocomposites for hydrogen production from wastewater.." *Polym. Adv. Technol.*, **34**, 1633 (2023).
2. H. K. Jaafar, A. Hashim, and B. H. Rabee, "Fabrication and unraveling the morphological, structural, and dielectric features of PMMA-PEO-SiC–BaTiO3 promising quaternary nanocomposites for multifunctional nanoelectronics applications.." *J. Mater. Sci., Mater. Electron.*, **35**, 128 (2024).
3. C. Malek, S. A. O. Abdallah, S. K. Awasthi, M. A. Ismail, W. Sabra, and A. H. Aly, "Biophotonic sensor for swift detection of malignant brain tissues by using nanocomposite YBa2Cu3O7/dielectric material as a 1D defective photonic crystal." *Sci. Rep.*, **13**, 8115 (2023).
4. R. K. Sendi, N. Al-Harbi, A. Atta, M. Rabia, and M. M. Abdelhamied, "Copper oxide and copper nanoparticles insertion within a PPy matrix for photodetector applications." *Opt. Quantum Electron.*, **55**, 956 (2023).
5. E. Abdeltwab and A. Atta, "Influence of ZnO nanoadditives on the structural characteristics and dielectric properties of PVA." *Int. J. Mod. Phys. B*, **35**, 2150310 (2021).
6. Z. A. Alrowaili, T. A. Taha, K. S. El-Nasser, and H. Donya, "Significant enhanced optical parameters of PVA-Y2O3 polymer nanocomposite films." *J. Inorg. Organomet. Polym. Mater.*, **31**, 3101 (2021).
7. G. A. Bastida, R. J. Aguado, M. V. Galván, M. Á. Zanuttini, M. Delgado-Aguilar, and Q. Tarrés, "Impact of cellulose nanofibers on cellulose acetate membrane performance." *Cellulose*, **31**, 2221 (2024).
8. A. Verma, R. Gupta, A. S. Verma, and T. Kumar, "Recent advances and challenges of conducting polymer-metal nanocomposites for the detection of industrial waste gases." *ECS J. Solid State Sci. Technol.*, **12**, 047002 (2023).
9. N. A. Althubiti, N. Al-Harbi, R. K. Sendi, A. Atta, and A. M. Henaish, "Surface characterization and electrical properties of low energy irradiated PANI/PbS polymeric nanocomposite materials." *Inorganics*, **11**, 74 (2023).
10. H. A. Al-Yousef, A. Atta, E. Abdeltwab, and M. M. Abdel-Hamid, "Structural characterization and dielectric properties of flexible PVA/PANI/Ag nanocomposite materials." *ECS J. Solid State Sci. Technol.*, **12**, 043006 (2023).
11. N. A. Althubiti, A. Atta, B. M. Alotaibi, and M. M. Abdelhamied, "Structural and dielectric properties of ion beam irradiated polymer/silver composite films." *Surface Innovations*, **11**, 90 (2022).
12. N. A. Alsaif, A. Atta, E. Abdeltwab, and M. M. Abdel-Hamid, "Fabrication, surface characterization and electrical properties of hydrogen-irradiated nanocomposite materials." *Surface Innovations*, **40**, 1 (2023).
13. M. R. El-Aassar, R. K. Sendi, A. Atta, N. Al-Harbi, M. Rabia, and M. M. Abdelhamied, "Characterization and linear/nonlinear optical properties of PVA/CS/TiO2 polymer nanocomposite films for optoelectronics applications." *Opt. Quantum Electron.*, **55**, 1212 (2023).
14. A. Bibi, A. Shakoor, N. A. Niaz, M. Raffi, and M. Salman, "Enhanced optical, electronic and dielectric properties of DBSA-doped polyaniline–calcium titanate composites.." *Bull. Mater. Sci.*, **46**, 185 (2023).
15. S. Fariha, M. S. Islam, M. Rockshat, S. U. Hani, J. Islam, H. M. Zabed, and F. I. Chowdhury, "Advances in PVC-based blend nanocomposites." *ECS J. Solid State Sci. Technol.*, **12**, 121005 (2023).
16. R. Sagar, A. P. Indolia, and M. S. Gaur, "Effect of carbon ions beam irradiation on structural and dielectric properties of Poly (vinylidene fluoride–trifluoroethylene) P

(VDF-TrFE) copolymer." *Nucl. Instrum. Methods Phys. Res., Sect. B*, **535**, 15 (2023).
17. B. M. Alotaibi, M. R. Atta, E. Abdeltwab, A. Atta, and M. M. Abdel-Hamid, "Surface modifications and optical studies of irradiated flexible PDMS materials." *Surface Innovations*, **12**, 73 (2024).
18. A. Atta, B. M. Alotaibi, and M. M. Abdelhamied, "Structural characteristics and optical properties of methylcellulose/polyaniline films modified by low energy argon irradiation." *Inorg. Chem. Commun.*, **141**, 109502 (2022).
19. R. K. Sendi, A. Atta, N. Al-Harbi, M. Rabia, and M. M. Abdelhamied, "Structural investigation and optical characteristics of low-energy hydrogen beam irradiated polyvinyl alcohol/polyaniline composite materials." *Opt. Quantum Electron.*, **55**, 1203 (2023).
20. A. Atta, N. Al-Harbi, B. M. Alotaibi, M. A. M. Uosif, and E. Abdeltwab, "Structural characteristics and dielectric properties of irradiated polyvinyl alcohol/sodium iodide composite films." *Inorg. Chem. Commun.*, **159**, 111651 (2024).
21. A. Al- Atta, B. M. Alotaibi, S. A. Waly, A. A. Reheem, and H. A. Al-Yousef, "Influence of argon irradiation on electrical properties of PVA/NaI polymer composites." *Surface Review and Letters (SRL)*, **31**, 1 (2024).
22. A. M. Abdel Reheem, M. M. Ahmed, M. M. Abdelhamid, and A. H. Ashour, "Verification of high efficient broad beam cold cathode ion source." *Rev. Sci. Instrum.*, **87**, 083302 (2016).
23. J. F. Ziegler, M. D. Ziegler, and J. P. Biersack, "SRIM–The stopping and range of ions in matter (2010)." *Nucl. Instrum. Methods Phys. Res., Sect. B*, **268**, 1818 (2010).
24. M. M. Abdelhamied, A. Atta, A. M. Abdelreheem, A. T. M. Farag, and M. A. El Sherbiny, "Argon ion induced variations in the structural and Linear/Nonlinear optical properties of the PVA/PANI/Ag nanocomposite film." *Inorg. Chem. Commun.*, **133**, 108926 (2021).
25. H. K. Patil, M. A. Deshmukh, S. D. Gaikwad, G. A. Bodkhe, K. Asokan, M. Yasuzawa, and M. D. Shirsat, "Influence of argon ions irradiation on polyaniline/single walled carbon nanotubes nanocomposite." *Radiat. Phys. Chem.*, **130**, 47 (2017).
26. S. Arif, F. Saleemi, M. S. Rafique, F. Naab, O. Toader, A. Mahmood, and U. Aziz, "Effect of silver ion-induced disorder on morphological, chemical and optical properties of poly (methyl methacrylate)." *Nucl. Instrum. Methods Phys. Res., Sect. B*, **387**, 86 (2016).
27. T. Taha and A. Saleh, "Dynamic mechanical and optical characterization of PVC/fGO polymer nanocomposites." *Appl. Phys. A*, **124**, 600 (2018).
28. N. A. Althubiti, A. Atta, N. Al-Harbi, R. K. Sendi, and M. M. Abdelhamied, "Structural, characterization and linear/nonlinear optical properties of argon beam irradiated PEO/NiO composite films." *Opt. Quantum Electron.*, **55**, 348 (2023).
29. Y. H. A. Fawzy, H. M. Abdel-Hamid, M. M. El-Okr, and A. Atta, "Structural, optical and electrical properties of PET polymer films modified by low energy Ar+ ion beams.." *Surf. Rev. Lett.*, **25**, 1850066 (2018).
30. Y. Maruko, T. G. P. Galindo, and M. Tagaya, "Modification of poly (dimethylsiloxane) by mesostructured siliceous films for constructing protein-interactive surfaces." *e-Journal of Surface Science and Nanotechnology*, **16**, 41 (2018).
31. A. Atta, Y. H. Fawzy, A. Bek, H. M. Abdel-Hamid, and M. M. El-Oker, "Modulation of structure, morphology and wettability of polytetrafluoroethylene surface by low energy ion beam irradiation." *Nucl. Instrum. Methods Phys. Res., Sect. B*, **300**, 46 (2013).
32. A. Biradar and J. Kandasamy, "A novel preparation and characterization of electroless NiP/MWCNT composite coated UHMWPE fabric in terms of wettability, electrical conductivity, thermal stability and breaking load resistance." *Mater. Chem. Phys.*, **299**, 127486 (2023).
33. A. Hassan, S. A. Abd El Aal, M. M. Shehata, and A. A. El-Saftawy, "Plasma-etching and modification of polyethylene for improved surface structure, wettability and optical behavior." *Surf. Rev. Lett.*, **26**, 1850220 (2019).
34. H. B. Baniya, R. P. Guragain, and D. P. Subedi, "Cold atmospheric pressure plasma technology for modifying polymers to enhance adhesion: a critical review." *Reviews of Adhesion and Adhesives*, **9**, 269 (2021).
35. D. K. Owens and R. C. Wendt, "Estimation of the surface free energy of polymers." *J. Appl. Polym. Sci.*, **13**, 1741 (1969).
36. E. Lugscheider, K. Bobzin, and M. Möller, "The effect of PVD layer constitution on surface free energy." *Thin Solid Films*, **355**, 367 (1999).
37. A. Atta and E. Abdeltwab, "Influence of ion irradiation on the surface properties of silver-coated flexible PDMS polymeric films." *Braz. J. Phys.*, **52**, 1 (2022).
38. N. M. Ainali, D. N. Bikiaris, and D. A. Lambropoulou, "Aging effects on low-and high-density polyethylene, polypropylene and polystyrene under UV irradiation: An insight into decomposition mechanism by Py-GC/MS for microplastic analysis." *J. Anal. Appl. Pyrolysis*, **158**, 105207 (2021).
39. M. M. Abdelhamied, A. M. Abdelreheem, and A. Atta, "Influence of ion beam and silver nanoparticles on dielectric properties of flexible PVA/PANI polymer composite films." *Plast. Rubber Compos.*, **51**, 1 (2022).
40. A. Hashim and A. Hadi, "Novel pressure sensors made from nanocomposites (biodegradable polymers–metal oxide nanoparticles): fabrication and characterization." *Ukr. J. Phys.*, **63**, 754 (2018).
41. A. Atta, M. M. Abdelhamied, A. M. Abdelreheem, and N. A. Althubiti, "Effects of polyaniline and silver nanoparticles on the structural characteristics and electrical properties of methylcellulose polymeric films." *Inorg. Chem. Commun.*, **135**, 109085 (2022).